# The Comparison of Bathymetric Estimation from Three High Resolution Satellite Imagery

**Samsul Bachri**
Institute Technology of Bandung (ITB)
**Muhammad Banda Selamat**
Bogor Agricultural University (IPB)
**Vincentius P Siregar**
Hasanuddin University (UNHAS)
**Sam Wouthuyzen**
LIPI

## ABSTRACT

**This study was using three high resolution satellite imagery to estimate bathymetric condition at shallow water coral reef environment around Pulau Panggang, Jakarta. The Worldview 2 supply 2 m spasial resolution with 8 spectral band, whereas Quickbird 2 produce 2.44 m spatial resolution in 4 spectral band and ALOS produce 10 m spasial resolution with also 4 spectral band. Red band of ALOS and Quickbird have high correlation with sand depth and the lowest are blue bands. Among this bands, Quickbird red band is the highest and its blue band is the lowest. Worldview visible bands may have low sand depth correlation because of noise from ripple wave during acquisition. This study shown that, Quickbird image is proven able to map water depth variation up to 8 metre at reef flat and lagoon area of Panggang island, Jakarta with RMSe is 1.1 metre. The result also shown an opportunity to implement this approach to bathymetric mapping of shallow water area at remote small islands.**

***Keywords :bathymetric estimation, high resolution imagery***

## 1 Introduction

Water depth (bathymetry) is an important factor to solve various coastal studies such as wave and current modelling, erosion, shoreline stability, sedimen propagation, port construction, thermal dispersion and maintenance of navigation routes. Collecting bathymetric data at a remote small islands are an expensive, time consuming and sometimes extremely difficult to conduct. For various reasons like wide area coverage, data dependency on depth and repetition, satellite images can be used to determine shallow water depth on these sites. Sometimes ground truth at selected locations is still needed to validate the bathymetric model produced by satellite imagery.

Depth water images acquired by remote sensing satellites consist of reflectance from water column and also atmosphere. Considering the case of water bodies, there will be significant change in the reflectance due to various parameters including water depth, dissolved matter and sea bed characteristics. Assuming the other two parameters uniform, it is obvious that the intensity of reflected electromagnetic energy will vary inversely with water depth. However, water depth variations are not easily distinguished from bottom color differences. Surface reflection effects add another element of confusion to the interpretation of the images.

The recent satellite imaging development promising a great challenge on this bathymetric mapping. Considering a new spectral band (ranging around ultraviolet to blue wave spectral region - called "coastal" band) on worldview 2 it hoping that visible satellite imaging may be use as an alternative to bathymetric mapping works on low to middle accuracy levels.

The main goal of this study is to evaluate the ability of two high resolution satellite image (eg Worldview and Quickbird) to on water depth mapping. The evaluation will based on depth penetration of visible bands of each satellite.

## 2 Background Theories

Lyzenga (1978) studies on mapping water depth conclude that the ratio algorithms for water depth and bottom features mapping are relatively simple and give acceptable results in many situations. The ratio algorithm can be develop to shallow water radiance model that involves effects of scattering in the atmosphere, reflection at the water surface as well as the components originating in the water itself.

Jupp (1988) develop depth zones theories based on a depth of penetration threshold for each band. Threshold values are determined from the maximum deep-water radiances, and for Landsat TM only six water depth zones or depth values can be derived. Although in some areas dark substrates such as sea-grasses may be misinterpreted as deep water, the technique is probably the most reliable for navigation purposes.

Bierwirth, et.al (1993) develop an algorithm to derived both substrate reflectance and water depth simultaneously. Their aim was to derive substrate reflectance factors in each band processed and, as a by-product, produce a continuous grey-scale depth image. At that stage of research, their assumed relatively clear water and only minor variations in the concentration of water column materials. The water attenuation coefficients were determined by regressing known bathymetric data against Landsat radiances. They assume that water column conditions were constant over the scene. The method was successfully tested in the Hamelin Pool area of Shark Bay, Western Australia. The errors are greatest for dark substrates which will resolve as deeper than true.

The studies on shallow water depth mapping were done using Quickbird images (Lyons et al. 2011), IKONOS (Stumpf et al. 2003; Lyzenga et al. 2006), SPOT (Melsheimer & Liew 2001; Lafon et al. 2002; Kao et al. 2009) and Landsat (Lyzenga 1981). The method used for bathymetric mapping may classified into two categories, empirical (Lyzenga 1978; Jupp 1988; Lafon et al. 2002; Gao 2009) and analytic / invertion (Dierssen et al. 2003; Su et al. 2008; Dekker et al. 2011). The common band use were blue and green band.

The fundamental principle behind using remote sensing to map bathymetry is that different wavelengths of light will penetrate water to varying degrees. When light passes through the water, it becomes attenuated by interaction with water column. The intensity of light, $I_d$, remaining after passage length p through water is formulated as:

$$I_d = I_0 . e^{-pk} \qquad \text{eq.1}$$

$I_0$= intensity of the incident light and
k= attenuation coefficient, which varies with wavelength

if vertical pathway of light from surface to bottom and back is assumed then p may be substituted by the term of 2d. where d is water depth. Then equation 1, may linierize by natural logarithm:

$$log_e\,(I_d) = log_e\,(I_0) - 2\,dk \qquad \text{eq.2}$$

Red light has a higher attenuation coefficient than green or blue, therefore it does not penetrate further than a few centimeter. The depth of penetration is depent on water turbidity. Dissolved materials in water will affects the depth of penetration because they scatter and absorb light, and so increase attenuation.

According to Benny and Dawson (1983), there are three assumptions to implement their algorithm: i) light attenuation is an exponential function of depth (equation 1), ii) water quality (the attenuation coefficient, k) does not vary within an image, iii) the color (reflective properties or albedo) of the substrate is constant. Assumption (ii) may or may not be valid for any image but has to be made unless supplementary field data are collected at the time of image acquisition. Assumption (iii) is certainly not true for many areas and will cause dense sea grass beds to be interpreted as deep water. Corrections to the final bathymetry chart could be made if a habitat map exists.

Even Jupp's method had same assumptions as Benny and Dawson's, but actually he made quiet different step to map water depth from satellite images. Jupp's method may implement by doing these steps : 1) the calculating depth of penetration (DOP) zones, 2) the interpolating depths within DOP zones, and 3) the calibrating depth within DOP zones.

Lyzenga's method applies water column correction to compensate the effect of variable depth (bathymetry) from different substrate. a transformation using natural logarithms will linearise the effect of depth on bottom reflectance. Theoretically, each bottom type should be represented by a parallel line, the gradient of which is the ratio of the attenuation coefficients for each band ($k_i/k_j$). It may say, for one of bottom type (e.g. sand), all pixels must lie along the same regression line. Those pixels further up the line have greater reflectance and are found in shallower water. Those pixels nearest the y-intercept are found in deeper water.

The y-intercept can be used as an index of bottom type. Relative depth can be inferred by the position of a pixel along a line of gradient $k_i/k_j$. Depth varies along the line so that the shallowest (brightest) pixels have the highest values, the deepest (darkest) pixels the lowest. Once the gradient $k_i/k_j$ is known, the axes of the bi-plot can be rotated through the angle θ, so that the new y-axis lies parallel to $k_i/k_j$. Positions of pixels along this new y-axis are indicative of depth.

Water depth calculated by an image is depth beneath a temporary water surface. This depth will depend on the height of the tide at the time of satellite overpass. Field depth data will also have been collected at different times of the day, at different points in the tidal cycle. Image and field depths must be unificated by reducing to depth datum. This tidal datum is normally calculated from the Lowest Astronomical Tide (LAT) level (the lowest point that the tide ever recedes to).

Similarly, the depth of water, z, measured in the field with an echo-sounder is equal to the depth below datum plus tidal height. The tidal height for each depth recording, must therefore be calculated and subtracted from the measured depth to give the depth of water below datum. Thus it is essential to record the time when each calibration depth is measured so that it can be corrected to datum later.

## 3 Methodology

The data for this study were collecting at Panggang island and its vicinity. The island may reach by boating around half an hour heading to the north from Jakarta. The equipments used during survey (January, 2012) were:

- 1 unit GPS MAP Sounder (freq. 50 kHz and 200 kHz)
- 1 unit Automatic Data Logger + software
- 1 unit laptop core2 duo
- 1 unit boat with 5 HP outboard engines
- 1 unit tide pole
- 1 unit steel chain with rope for transducer calibration
- 1 unit digital camera for documentation

Due to sea wave characteristics, some corrections must be apply to water depth measured. These corrections are: 1) equipment default correction, this value obtained by transducer calibration, and 2) tide correction, which obtained by tidal observation coincident with sounding work. The relationship between depth measured, depth corrected and its corrected values is shown in Figure 1.

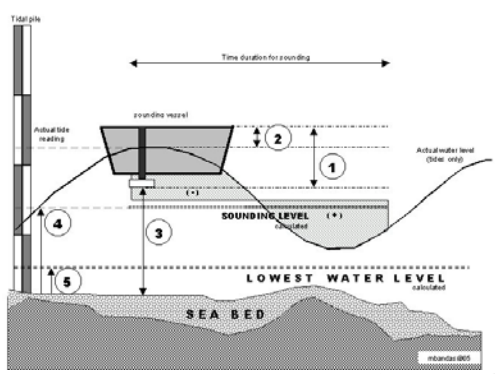


Figure 1. Corrections to Depth Measured

Three different satellite images were use for this study. The images description are shown at Table 1 and 2. The visualization of natural composite image from three satellites are shown in Figure 2.

Table 1. Satellite images used in this study

| Satellite | Bands | Spatial Resolution | Acquisition |
|---|---|---|---|
| Worldview 2 | 8 | 2.07 m | October 19, 2011 |
| Quickbird 2 | 4 | 2.44 m | September 28. 2008 |
| ALOS AVNIR 2 | 4 | 15 m | September 15. 2008 |

Table 2. Sensor characteristics of Worldview, Quickbird and ALOS AVNIR 2 satellites (modificated from Digital Globe, 2010 and JAEA, 2008)

| Spectrum | Wave length (nm) | | |
|---|---|---|---|
| | Worldview 2 | Quickbird 2 | AVNIR 2 |
| Coastal | 400 - 450 | | |
| Blue | 450 - 510 | 430 - 545 | 420 – 500 |
| Green | 510 - 580 | 466 - 620 | 520 – 600 |
| Yellow | 585 - 625 | | |
| Red | 630 - 690 | 590 - 710 | 610 – 690 |
| Red Edge | 705 - 745 | | |
| Near IR | 770 - 895 | 715 - 918 | 760 – 890 |
| Near IR | 860 - 1040 | | |

### *Creating Depth of Penetration (DOP) Zones (Jupp, 1988)*

Digital Number data require either dark pixel subtraction or some other form of atmospheric correction. All infrared bands removed and land areas masked out.

1) choose an area of deep water with properties we believe to be typical for the area
2) Calculate the maximum, minimum and mean deep water pixel for each band. Let the minimum in band *i* be $L_{i\ deep\ min}$, the maximum $L_{i\ deep\ max}$ and the mean $L_{i\ deep\ mean}$
3) if a pixel value in band *i*, $L_i$, is > $L_{i\ deep\ max}$ then some light in band *i* is being reflected from the seabed to the sensor. The depth is therefore less than the maximum depth of penetration, denoted by $z_i$ for band *i*. If, for the same pixel, $L_{ij}$, is > $L_{j\ deep\ max}$ , then the depth of that pixel is between $z_i$ and $z_{ij}$.
4) a few error pixels will have higher values in some band, which should not happen in theory. They may be coded to zero and filtered out of the final depth image.

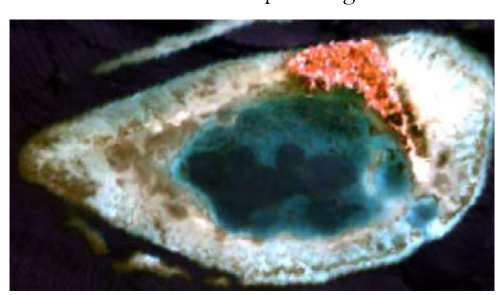

(a)

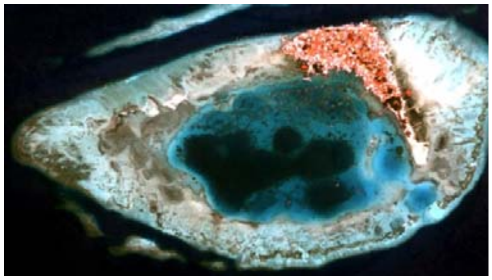

(b)

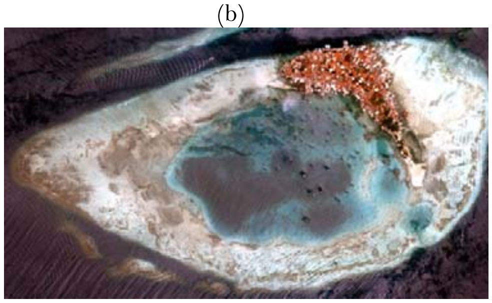

(c)

Figure 2. Natural composite images of study area: a) ALOS AVNIR, b) Quickbird 2 and c) Worldview 2

### *Interpolating DOP Zones*

1) DOP images then may be used to make DOP zone masks for all bands. All pixels within DOP zone 1 coded to a value of 1 and all other pixels in the image to 0, and repeating with other DOP zones.
2) Multiply the original image by each DOP zone masks. Data in pixels outside the DOP zone will be recorded to 0.
3) Estimate $L_{i\,max}$ and $L_{i\,min}$ for each DOP zone $i$. $X_{i\,min}$ and $X_{i\,max}$ can then be calculated since $L_{ideepmean}$ is known. The $A_i$ can then be calculated from equation 3 and 4.

$$k_2 = \frac{X_{2\,max} - X_{2\,min}}{2(z_2 - z_3)} \qquad \text{eq. 3}$$

$$A_2 = X_{2\,min} + 2k_2 z_2 \qquad \text{eq. 4}$$

4) Using equation 5 to assign depth for each pixel in each DOP. This will produces separate interpolated DOP depth images. These are added together to produce a depth image for the area of interest.

$$z = \frac{A_i - X_i}{2k_i} \qquad \text{eq. 5}$$

### *Calibration of DOP zones*

1) Depth data typically consist of echo sounder readings at a series of positions. Calculate which sites lie within each DOP and plot frequency distribution histograms of known depths in each DOP
2) Jupp indicates that the point of intersection between histograms is the best decision value for the depth separating each DOP zone.
3) new values of Zj, ki and Ai are calculated and equation 5 written to assign depths to each pixel in each DOP

### *Accuracy Assessment*

Simple regression between depth pair of data could be implement to estimate how accurate this method in water depth mapping. The regression equation also will portray the level of confidence of the final bathymetric map for area of interest.

## 4 Result and Discussion

Geomorphic zonation at coral reef environment usually associated to depth profile. Hence it presentation is spatially easy to detect by moderate satellite resolution such Landsat, SPOT and ASTER. According to Mumby and Harborne (1999) geomorphic zone has clear boundary between them due to depth differences so it is easy to identified by using visible band combination from satellite images. Blanchon (2011) could recognize reef flat, reef lagoon, reef front and reef slope from high resolution Quickbird satellite image.

The crossectional and top view of coral reef environment at Panggang island is shown at Figure 3. The water depth profile is provided by echo sounding and already reduced to tidal datum. From this figure we could recognize some geomorphic zonation, such as reef crest, reef flat and lagoon. Note the lagoon is almost 15 metre depth, whereas reef flat depth is only around 1 to 2 metre.

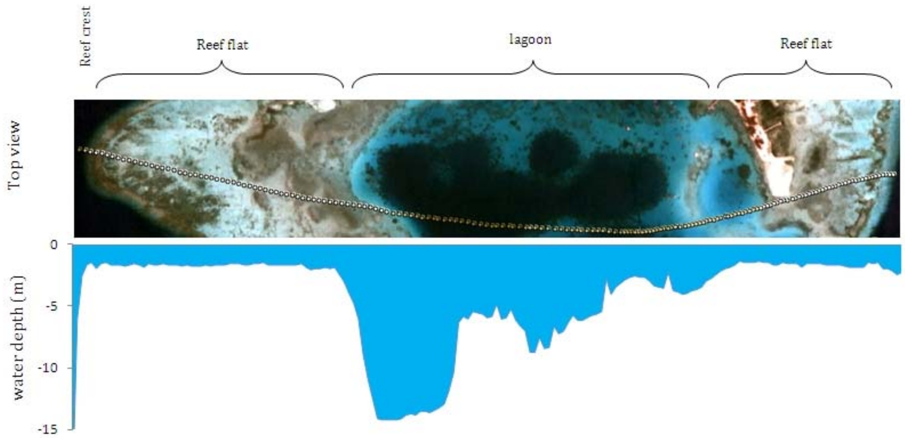


Figure 2. Geomorphic zonation of Panggang reef waters

It is obvious that bottom substrate like sand have good relationship with depth variation. Common substrates in reef environment are sand, seagrasses and coral reef. We evaluate sand relationship with waterdepth by extracting its correspondence digital value from ALOS, Quickbird and worldview images. Figure 3 shows us that, even Worldview has great spatial resolution compare to ALOS and Quickbird, but in this case it has very low coefficient determination hence not representative to bathymetric image processing.

Red band of ALOS and Quickbird have high correlation with sand depth and the lowest are blue bands. Among this bands, Quickbird red band is the highest and its blue band is the lowest. From this fact we may get a brief description that if use Jupp's algorithm to predict bathymetry from ALOS images, we may have three DOP (depth penetration zone) because its three bands have good relationship with sand depth. Meanwhile, if use Quickbird image, we only have two DOP wich are from green and red bands only.

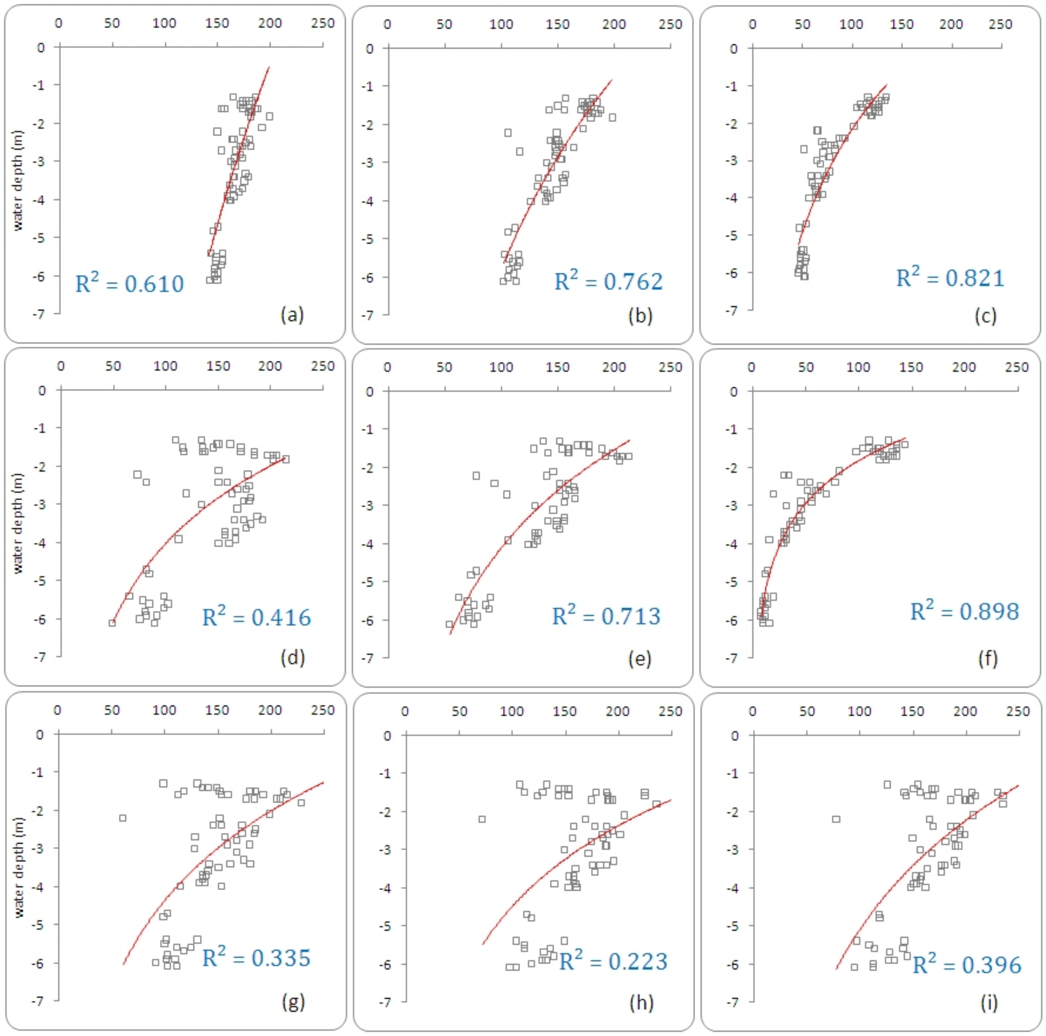


Figure 3. Digital number comparison of sand depth from band 1, 2 and 3 of ALOS (a, b, c), Quickbird (d, e, f) and Worldview (g, h, i) respectively

We re-evaluate worldview image due its low sand depth correlation value and found that the image also record ripple wave during acquisition. So this noise may affected every digital number of visible bands we use and contribute to low value of sand depth correlation.

Considering to sand depth correlation values, we decide to use Quickbird image to produce bathymetric image by implement Jupp's algorithm. The Jupp's algorithm paremeters are shown at Table 2. The DOP (depth penetration values) of band 2 is actually acting as boundary level for depth more than 2 metre, whereas DOP of band 3 was use for delineating depth area less than 2 metre. Ki and Ai coefficient are needed to solve depth estimation by using equation 5. The result of Jupp's algorithm implementation is shown in Figure 5.

Table 2. Summary of Jupp Parameters for Quickbird image

| Parameters | band | |
|---|---|---|
| | 2 | 3 |
| DOP 2 | 42 - 53 | |
| DOP 3 | | 8 - 131 |
| Parameters | band | |
| | 2 | 3 |
| ki | 0.114536 | 0.034657 |
| Ai | 5.045528 | 1.386294 |

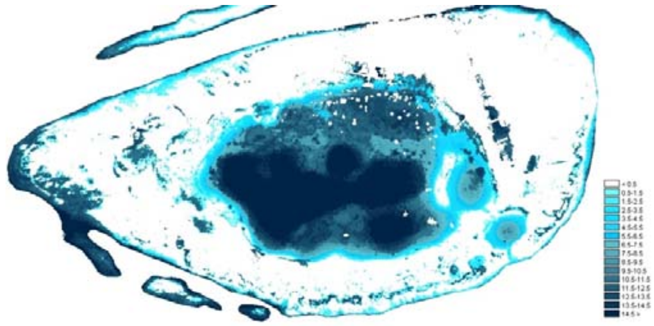

Figure 5. Bathymetric image from Quickbird

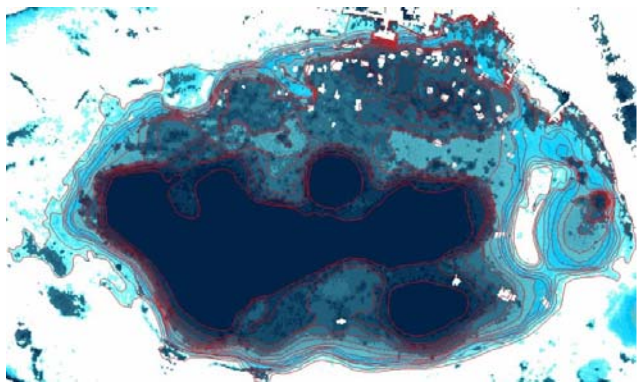

Figure 6. Tracing bathymetric contour from Quickbird bathymetric image

To measure the accuracy of this bathymetric map, some point was carried out on both field depth values and bathymetric image. The pair of depth values then plotted in to cartesian diagram to get a general formulation of the regression. The determination coefficient describes the reliability of the model, the bigger the value the more reliable is (Figure 7a).

In statistical view, this model is able to describe almost 78 percent of any values given in data set. This means if we get a value say 2 meter from bathymetric image, then we should note that the real value maybe around 1 to 3 meters depth. The predicted water depth profile shown in Figure 7b, where it gives a more clear explanation about the accuracy of bathymetric image. The root mean square error (RMSe) for each pair of water depth (image and field) is around 1.1 metre for a maximum 9 metre depth.

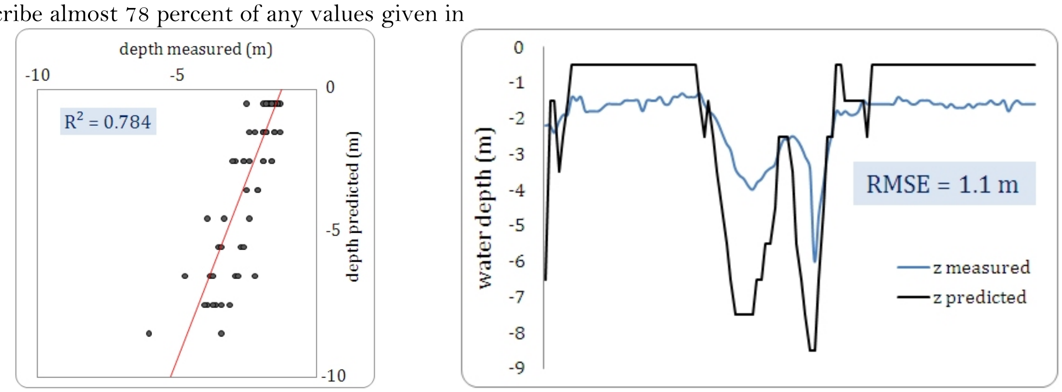


(a) (b)

Figure 7.

The final product from Jupp's algorithm is not just bathymetric image as shown in Figure 5. By draping its raster image to bathymetric countour (Figure 6) then we get some kind of digital bathymetric terrain model (Figure 8). So then we may say that for the sake of simplicity, this methodology can be very valuable for bathymetric mapping especially in surf zone area where conventional method is hard to implement.

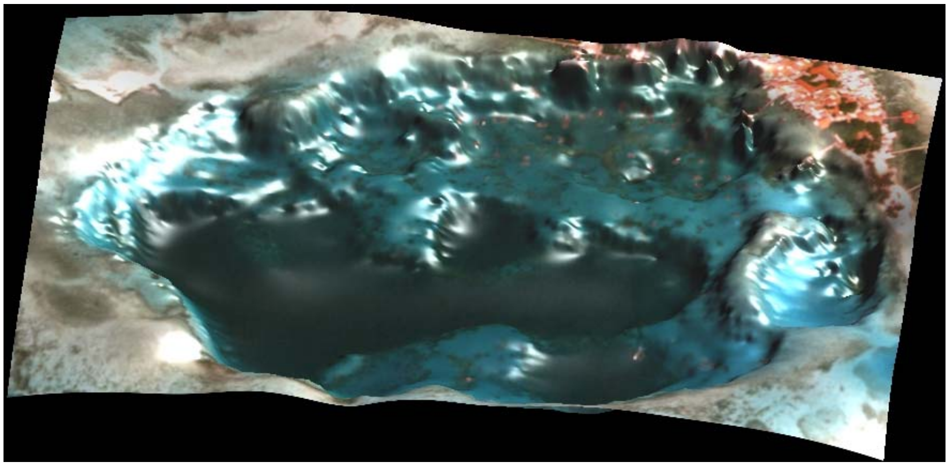

Figure 8. Digital bathymetric terrain model of Panggang island

## 5 Conclusion

In clear shallow water coral reef areas (e.g remote small island), the optic sensor of satellite imagery promising an opportunities as a source of bathymetric mapping technology. This study shown that, Quickbird image is proven able to map water depth variation up to 9 metre at reef flat and lagoon area of Panggang island, Jakarta. Eventough the RMSe is 1.1 metre, but the potray of bathymetric terrain may give a valuable information for some application such as sea current modelling, predicting fish juvenil migration along seagrass and coral reef habitat.

## REFERENCES


Benny, A.H and Dawson, G.J. 1983. Satellite Imagery as an aid to bathymetric charting in the Red Sea. The Cartographic Journal. 20 (1), 5-16.

Bierwirth, P.N, T Lee and R V Burne. 1993. Shallow Sea-Floor Reflectance and Water Depth Derived by Unmixing Multispectral lmagery. Photogrammetric Engineering & Remote Sensing, Vol.59, No.3, 331-338.

Blanchon P. 2011. Geomorphic zonation. Di dalam: David H, editor. Encyclopedia of Modern Coral Reefs. Springer Science.

Dekker AG et al. 2011. Intercomparison of shallow water bathymetry, hydro-optics, and benthos mapping techniques in Australian and Caribbean coastal environments. Limnol Oceanogr. 9: 396–425.

Dierssen HM, Zimmerman RC, Leathers RA, Downes TV, Davis CO. 2003. Ocean color remote sensing of seagrass and bathymetry in the Bahamas Banks by high-resolution airborne imagery. Limnol Oceanogr 48(1 part 2):444–455.

Digital Globe, 2010. White Paper. The Benefits of the 8 Spectral Bands of WorldView-2. Digitalglobe

JAEA, 2008. ALOS Data Users Handbook. Revision C. Earth Observation Research and Application Center

Gao J. 2009. Bathymetric mapping by means of remote sensing: methods, accuracy and limitations. Progr. in Physic. Geogr. 33(1):103–116.Jupp, D.L.B. 1988. Background and Extentions to Depth of Penetration (DOP) mapping in shallow coastal waters. Proceedings of the Symposium on Remote Sensing of the Coastal Zone, Gold Coast, Queensland, September 1988, IV.2.1 – IV.2.19.

Kao HM, Ren H, Lee CS, Chang CP, Yen JY, Lin TH. 2009. Determination of shallow water depth using optical satellite images. Int. J. Remote Sensing 30(23): 6241–6260.

Lafon V, Froidefond JM, Lahet F, Castaing P. 2002. SPOT shallow water bathymetry of a moderately turbid tidal inlet based on field measurements. Remote Sen. of Environ. 81: 136– 148.

Lyons M, Phinn S, Roelfsema C. 2011. Integrating Quickbird multi-spectral satellite and field data: mapping bathymetry, seagrass cover, seagrass species and change in moreton bay, australia in 2004 and 2007. Remote Sens. 3: 42-64.

Lyzenga, D.R. 1978. Passive Remote Sensing Techniques for Mapping Water Depth and Bottom Features. Applied Optics, 17, 379-383.

Lyzenga DR. 1981. Remote sensing of bottom reflectance and water attenuation parameters in shallow water using aircraft and landsat data. Int. J. Remote Sensing 2(1):71-82.

Lyzenga, DR, Malinas NP, Tanis FJ. 2006. Multispectral bathymetry using a simple physically based algorithm. IEEE Trans. on Geosci. and Remote Sens. 44(8):2251-2259.

Melsheimer C, Liew SC. 2001. Extracting bathymetry from multi-temporal SPOT. Paper presented at the 22nd Asian Conference on Remote Sensing, 5-9 November 2001, Singapore.

Mumby PJ, Harborne AR. 1999. Development of a systematic classification scheme of marine habitats to facilitate regional management and mapping of Caribbean coral reefs. Biologic. Conserv. 88:155-163.

Stumpf RP, Holderied K, Robinson JA, Feldman G, Kuring N. 2003a. Mapping water depths in clear water from space. Proceedings of the 13th Biennial Coastal Zone Conference.Su et al. 2008